JPE 13-1-6

http://dx.doi.org/10.6113/JPE.2013.13.1.51

Analysis and Design of a New Topology of Soft-Switching Inverters

Rong Chen† and Jia-Sheng Zhang*

†*College of Information and control Engineering, China University of Petroleum, Qingdao, China

Abstract

This paper proposes the power conversion mechanism of a bailer-charge-transfer zero-current-switching (CT-ZCS) circuit. The operation modes are analyzed and researched using state trajectory equations. The topology of CT-ZCS based on soft-switching inverters offers some merits such as: tracking the input reference signal dynamically, bearing load shock and short circuit, multiplying inverter N+1 redundancy parallel, coordinating power balance for easy control, and soft-switching commutation for high efficiency and large capacity. These advantages are distinctive from conventional inverter topologies and are especially demanded in AC drives: new energy generation and grid, distributed generation systems, switching power amplifier, active power filter, and reactive power compensation and so on. Prototype is manufactured and experiment results show the feasibility and dynamic voltage-tracking characteristics of the topology.

Key words: Bailer-charge-transfer, Double-digit three-state interlocking comparison pulse density modulation (DTIC-PDM), Topology, Trajectory of state, Zero-current-switching

I. INTRODUCTION

In recent years, a variety of voltage wave inverter such as switch-linearity hybrid (SLH) power converters [1], [2], voltage tracking switching power amplifiers (SPAs) [3], high frequency link inverters [4]-[6] and resonant soft switching inverters [7], [8] have been proposed to overcome the drawbacks of the power conversion based on the conventional PWM waveform generation mechanism, especially in bridge inverters; however, there are still various defects. The purpose of this paper is to investigate the PWM waveform generation mechanism, and to present a voltage tracking inverter topology based on the bailer-charge-transfer zero-current-switching (CT-ZCS) and a dedicated pulse density modulation (PDM) control method. The output voltage of the topology shows good dynamic tracking performances with the input reference signal as linear power amplifier and a good output waveform which the output signal can track the input reference signal without any difference. The inverter based on the CT-ZCS offers more advantages than that of the conventional bridge topology.

Manuscript received Apr. 6, 2012; revised Nov. 18, 2012
Recommended for publication by Associate Editor Joung-Hu Park.
†Corresponding Author: chenrongjn@163.com
Tel: +86-532-8698-3023, Fax: +86-532-8698-1335, China Univ. of Petroleum
*College of Information and control Engineering, China University of Petroleum, China

II. CIRCUIT TOPOLOGY AND TRANSFORMATION MECHANISM OF CT-ZCS

The disadvantages of conventional converters such as boost, buck-boost, sepic [9] and zeta which accomplish the power conversion by using the energy storage inductor are the large volume of the inductor and the low power factor. Power conversion using an energy storage capacitor provides advantages such as small volume, low loss and excellent electromagnetic compatibility. Series resonant converters (SRCs) [10] have the characteristics of zero-current soft-switching and can generate the high-frequency current pulse sequences using the energy storage capacitor. Fig. 1 shows the principle of the CT-ZCS DC/DC conversion

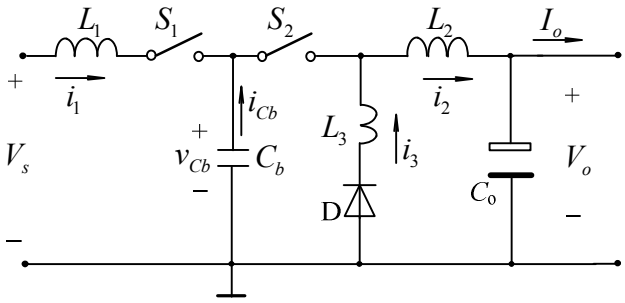

Fig. 1. Principle of CT-ZCS converter.

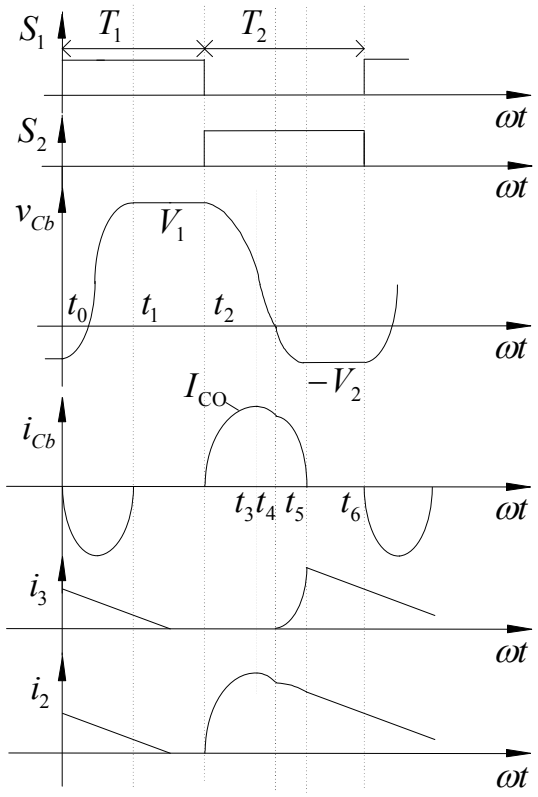

Fig. 2. Waveforms of CT-ZCS converter.

topology.

The input side draws energy from the DC power by the resonant way and the output side transfers the energy (charge) to the output capacitor C_o and load by using the resonant current pulse. The charge-transfer frequency of the bailer capacitor C_b and the discrete high-frequency current pulse chain which charge C_o are modulated according to the on-off alternation of two power switches. Two power alternative switches between the input and output both work in zero current switching mode, which helps to reduce the switching losses and improve efficiency. By regulating the density of the discrete current pulse, the output voltage and power can be changed.

In Fig. 1, assuming that the switch S_1 and switch S_2 are ideal power switches, they are in the alternative state, when the values of the two capacitors meet C_o>>C_b. In a switching period T, the topology of a CT-ZCS converter can be divided into several equivalent sub-circuit topologies the corresponding voltage and steady state current waveforms are shown in Fig .2,where T_1, T_2 are respectively the driving signal duration on S_1, S_2, T_1+T_2=T.

Mode 0 [t_0, t_1]: The switch S_1 is turned on at t_0, and C_b begins to resonate with L_1 and charge. Energy from the V_s is transferred to C_b through L_1 and S_1. This mode ends when the voltage of C_b (V_{Cb}) reaches the maxium value V_1 (where V_1 must be greater than V_s) and S_1 turns off with ZCS. The initial condition is $v_{Cb}(0)$=−V_2. This state maintains until t_2.

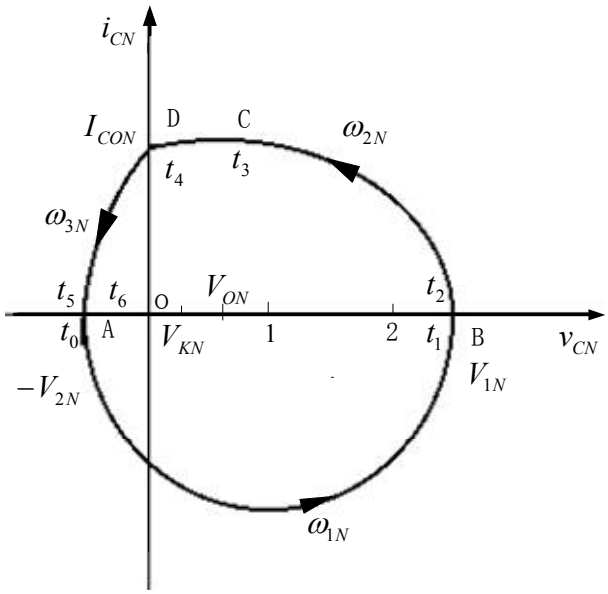

Fig. 3. State trajectory of CT-ZCS converter with DCM.

Mode 1 [t_2, t_4]: At t_2, S_1 is off and S_2 is turned on. C_b begins to resonate with L_2 and C_o. Due to C_o>>C_b, C_o is equivalent with the constant voltage source. This mode ends when the voltage across C_b, V_{Cb}, reaches zero and the diode D turns on. Energy in the bailer capacitor C_b is transferred to the load and C_o through S_1 and L_2.

If S_1 is a fast thyristor, the time between ZCS of S_1 and the moment V_1 drops below V_s must be greater or equal to off of the thyristor.

Mode 2 [t_4, t_5]: At t_4, V_{Cb} reaches zero and D starts to conduct as C_b continue to resonate with L_2 and C_o and the voltage across it becomes negative. This mode ends when V_{Cb} reaches the negative peak value, -V_2. Energy in the inductor L_2 is transferred to the load and C_o.

Mode 3 [t_5, t_6]: At t_5, the switch S_2 is turned off with ZCS and D is still on. The current through L_2 and L_3 decreases linearly. At t_6, the current through L_2 may be continued to decrease. At the end of this mode, S_1 is turned on and this begins the beginning of a similar switching of half cycle.

Analysis above shows that S_1, S_2 and D can turn on and off softly with ZCS. Capacitor C_b plays a dual role: 1) as a zero current switching resonant component to ensure power device has a lower *di/dt* during the state of turning on and off, and 2) as the core component to transfer energy from V_s to V_o. If the pulse density is controlled by the power switch, which is called pulse density modulation (PDM) method, the amplitude of the output voltage or current can be changed.

III. THE STATE TRAJECTORIES OF CT-ZCS CONVERSION TOPOLOGY

The advantages of the state trajectories is its convenience in the quantitative calculation and intuitive analysis. The

standardized parameters are given as below [11], [12].

Standardized voltage: $V_{ON}=V_O/V_S=\lambda$, $v_{CN}=v_{Cb}/V_S$. V_{ON} and v_{CN} are respectively standardized output voltage and standardized capacitor voltage.

Standardized current: $i_{CN}=i_{Cb}\cdot Z_1/V_S$, $I_{ON}=I_O\cdot Z_1/V_S$ and $Z_1=\sqrt{L_1/C_b}$.

Standardized frequency:

$\omega_{1N}=\omega_1/f$, $\omega_{2N}=\omega_2/f$, $\omega_{3N}=\omega_3/f\cdot\omega_1=1/\sqrt{L_1C_b}$, $\omega_2=1/\sqrt{L_2C_b}$ and $\omega_3=1/\sqrt{L_2L_3C_b/(L_2+L_3)}$ are the three circuit resonant angular frequency respectively. $f=1/T$ is switching frequency.

The state trajectories will be determined respectively by the current through L_2, which is discontinuous or continuous.

In the case of the current through L_2 being discontinuous, the dynamic process of resonant state variables when the CT-ZCS converter is in the steady-state can be expressed by the state trajectory on the i_{CN}~v_{CN} plane which is shown in Fig. 3. The state point starts from point A $(t=t_0)$, moves along the curves AB, BCD and DA, and returns to point A. The closed trajectory curve is formed and a switching cycle is finished.

Mode 0 [t_0, t_1]: The state trajectory curve AB segment in Fig. 3 moves along with the semi-circular arc with the center point (1,0) and reaches B at t_1.

The state equation and standardized state trajectory equation are expressed as

$$\begin{bmatrix}\dot{v}_{Cb}\\ \dot{i}_{Cb}\end{bmatrix}=\begin{bmatrix}0 & -\frac{1}{C_b}\\ \frac{1}{L_1} & 0\end{bmatrix}\begin{bmatrix}v_{Cb}\\ i_{Cb}\end{bmatrix}+\begin{bmatrix}0\\ -\frac{1}{L_1}\end{bmatrix}V_s \tag{1}$$

$$(v_{CN}-1)^2+i_{CN}^2=\rho_1^2 \quad (\rho_1=\sqrt{(V_{CON}-1)^2+I_{LON}^2}) \tag{2}$$

The state point stays at point B before t_2. V_{CON} and I_{LON} are respectively the standardized initial value of capacitor voltage and the current through L_2. The radius of the semi-circle trajectory is ρ_1 which is determined by the initial value.

Mode 1 [t_2, t_4]: The state equation and standardized state trajectory equation are expressed as

$$\begin{bmatrix}\dot{v}_{Cb}\\ \dot{i}_{Cb}\end{bmatrix}=\begin{bmatrix}0 & \frac{-1}{C_b}\\ \frac{1}{L_2} & 0\end{bmatrix}\begin{bmatrix}v_{Cb}\\ i_{Cb}\end{bmatrix}+\begin{bmatrix}0\\ \frac{-1}{L_2}\end{bmatrix}V_O \tag{3}$$

$$(v_{CN}-V_{ON})^2+K_1i_{CN}^2=\rho_2^2 \quad (\rho_2=\sqrt{(V_{CON}-V_{ON})^2+K_1I_{CON}^2}) \tag{4}$$

The state trajectory curve BD segment in Fig. 3 moves along with the elliptical arc with the center point (V_{ON}, 0). The semi-major axis is ρ_2. Semi-minor axis is $\sqrt{1/K_1}\cdot\rho_2$, where $K_1=L_2/L_1$ and $K_1\geq 1$.

Mode 2 [t_4, t_5]: The governing equation of this mode is $K_2=L_3/(L_2+L_3)$, $V_{KN}=K_2V_{ON}$ and $I_{KN}=\sqrt{K_1K_2}\cdot I_{CON}$.

The state trajectory curve DA segment in Fig. 3 moves along with the elliptical arc with the center point (V_{KN},0). The semi-major axis is $\rho_3/\sqrt{K_1K_2}$, and the semi-minor axis is ρ_3.

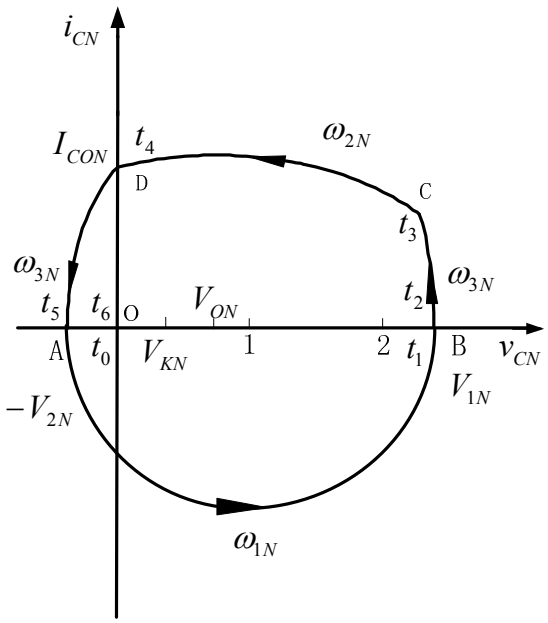

Fig. 4. State trajectory of CT-ZCS converter with CCM.

The state equation and the standardized state trajectory equation are expressed as

$$\begin{bmatrix}\dot{v}_{Cb}\\ \dot{i}_{Cb}\end{bmatrix}=\begin{bmatrix}0 & \frac{-1}{C_b}\\ \frac{L_3+L_2}{L_3L_2} & 0\end{bmatrix}\begin{bmatrix}v_{Cb}\\ i_{Cb}\end{bmatrix}+\begin{bmatrix}0\\ \frac{-1}{L_2}\end{bmatrix}V_O \tag{5}$$

$$(v_{CN}-V_{KN})^2+(\sqrt{K_1K_2}i_{CN})^2=\rho_3^2 \quad (\rho_3=\sqrt{V_{KN}^2+I_{KN}^2}) \tag{6}$$

The state point stays at point A before t_6.

If the current through L_2 is continuous, the continuous current mode will occur when the current through L_2 decreases slowly and cannot be reduced to zero after a period. There is a slight difference in *Mode* 1 [t_2, t_4]. Its state trajectory curve is shown in Fig. 4.

IV. Parameter Calculation and Analysis

The calculation methods of the main parameters about CT-ZCS and the CT-ZCS DC-DC converter circuit constraints can be obtained in [13].

In the working process of CT-ZCS converters, the maximum voltage across the capacitor C_b should be given a particular concern, because the excessive capacitor voltage will have high demands on the breakdown voltage. It can be seen from state trajectories shown in Fig. 3, under the steady-state operation, that the maximum forward standardized voltage value of v_{Cb} is V_{1N} and the largest negative standardized voltage value of v_{Cb} is V_{2N}. Under the condition of ignoring the resonant loss, the expression between V_{1N} and V_{2N} is

$$V_{1N}=V_{2N}+2 \tag{7}$$

The standardized voltage values V_2 directly determines the maximum forward standardized voltage values V_1. Based on the capacitor ampere-second balance principle and state trajectory, the calculation method of V_2 is derived.

As shown in Fig 3,

$$\rho_3 = \rho_1 - 1 + V_{KN} \tag{8}$$

$$\rho_1 = V_{2N} + 1 \tag{9}$$

$$\rho_2 = \rho_1 + 1 - V_{ON} \tag{10}$$

From (1) through (6)

$$\begin{cases} K_2^2\lambda^2 + K_1K_2I_{CON}^2 = (V_{2N} + K_2\lambda)^2 \\ \lambda^2 + K_1I_{CON}^2 = (V_{2N} + 2 - \lambda)^2 \end{cases} \tag{11}$$

where $\lambda = V_{ON}$, according to the relationship above, we can obtain the following results

$$V_{2N} = 2(\beta + \sqrt{\beta^2 + \beta}) \tag{12}$$

$$I_{CON} = \sqrt{\frac{V_{1N}^2 - 2\lambda V_{1N}}{K_1}} \tag{13}$$

where $\beta = (1-\lambda)L_3 / L_2$, from (12), if the direct current transfer ratio satisfies $\lambda=1$ and $V_2=0$ (if $\lambda=0$, $V_2=V_{2N}$). V_{2N} is closely related with L_3. In order to reduce the capacitor voltage, $L_3<<L_2$ is usually chosen.

If the condition of the current through L_2 is discontinuous, V_2 is related with V_o, and is not with I_o. Whereas, in the case of the current through L_2 is continuous, V_2 is also related with I_o. If I_o increases, so does V_2.

Based on the equation (6), (8) and (9), combining with the current waveform in the continuous mode, the expression can be expressed as

$$I_{CO} \approx \frac{V_O}{L_2 + L_3} \cdot \frac{T}{2} + I_O \tag{14}$$

$$V_2 = \sqrt{K_2^2V_O^2 + \frac{L_2}{C_b}K_2\left(\frac{V_OT}{2(L_2+L_3)} + I_O\right)^2} - K_2V_o \tag{15}$$

Under the ideal conditions, ignoring the converter losses, from (7), the energy transfer to the output load during a steady-state cycle is deduced as

$$W_T = \frac{1}{2}C_b(V_1^2 - V_2^2) = 2C_bV_S(V_2 + V_S) \tag{16}$$

Therefore, as the output voltage and output current are obtained, the charge transfer frequency is given as

$$f = \frac{V_OI_O}{2C_bV_S(V_2 + V_S)} \tag{17}$$

where V_2 is determined by (12) with discontinuous current mode. V_2 is related with I_o and f. Supposing the output voltage and output current are obtained, f can be obtained from (16) and (17).

Assuming that the output load current is constant, under the closed loop voltage control of PDM, the output voltage increment from the transferred energy is ΔV_O, based on (16) and the per cycle charge transfer energy balance relationship, the maximum output voltage ripple is shown as follows

$$\Delta V_{O\max} \approx (V_1 - V_2)C_b / C_O \tag{18}$$

If the voltage transfer ratio is constant and $C_o>>C_b$, the output ripple is very small.

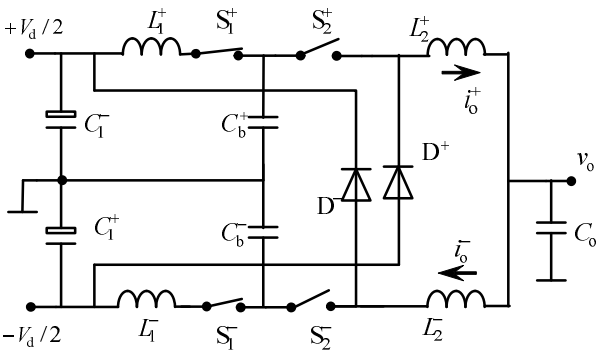

Fig. 5. CT-ZCS inverter topology.

V. VOLTAGE TRACKING CT-ZCS INVERTER TOPOLOGY

The AC frequency converter using the hysteresis current tracking control method [14] can make the stator current track change the given reference signal dynamically. It offers the advantages of fast tracking response and excellent waveforms. Its working mechanism is to exert the discrete voltage pulses sequence with positive and negative polarity on the inductor; the inductor current is characterized by the alternating positive and negative variations. Under the condition of the appropriate control of the polarity and the width of the voltage pulse based on closed-loop control, the inductor current can track the given reference signal change automatically. If the hysteresis width is small enough, the change of the inductor current is almost proportional to the change of the given reference signal. According to the circuit duality principle, we can exert the discrete current pulse sequence with positive and negative polarity on the capacitor to construct a voltage tracking converter topology, and the capacitor voltage can track the change of the given reference signal. As a result, how to obtain a controllable discrete current pulse sequence with polarity and width becomes the key issue [15].

The CT-ZCS DC conversion topology in Fig. 1 is used as the component unit. The cross-connection with two complementary symmetry (output positive and negative current pulse sequences) topology units is considered. The outputs of two units are connected together, which put an effect on the public output capacitor C_o and load, and control the output capacitor voltage to rise (charging) or to fall (discharge) respectively. Therefore, a soft switching voltage tracking CT-ZCS inverter topology is obtained as shown in Fig. 5.

The value of the soft switching resonant inductor in CT-ZCS inverter topology decreases with the increase of switching frequency. Compared with the conventional converters based

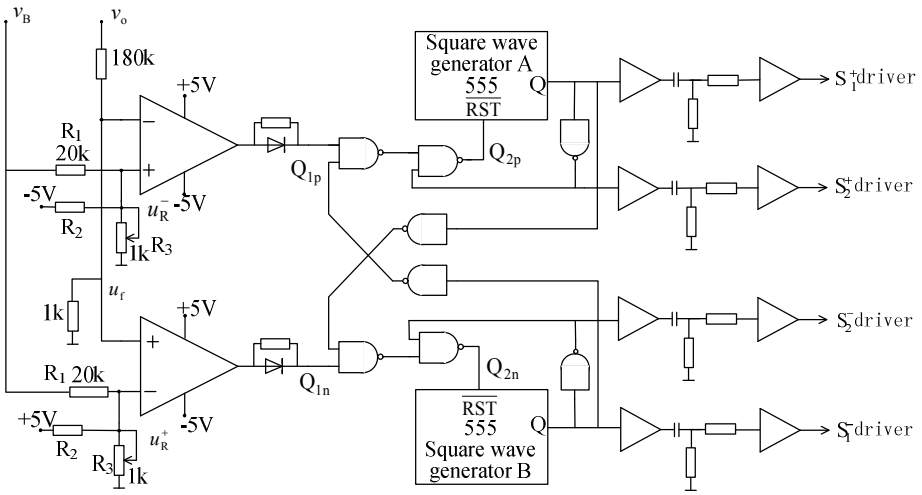

Fig. 6. Control circuit of CT-ZCS inverter based on DTIC-PDM.

on the energy storage inductor， the energy transferring mechanism based on the bailer-capacitor has such advantages as small volume, low loss, cost savings, and good electromagnetic compatibility, etc. Furthermore, it also has many characteristics, such as tracking the input reference signal dynamically and replicating it in proportion to its value accurately, bearing load shock and short circuit, multiple inverter N+1 redundant parallel and power balance coordination easy control, and the efficient high-capacity comes from the soft-switching commutation technology. These advantages have been confirmed by the DC arc welding power supply and the short-circuit experiment composed of the CT-ZCS DC-DC converter. Owing to the CT-ZCS inverter resonant zero current switching mechanism [16], a fast thyristor can be used as the switching device, and it has no short circuit on one of the arms as the conventional bridge inverter, making it more appropriate for expansion of output capacity, reducing costs and improving reliability. In an AC variable frequency variable speed drive system based on the CT-ZCS inverter, the sinusoidal current waveform, the flux locus and the low-frequency speed running performance of the motor will achieve a qualitative improvement.

The reactive energy exchange between the inverter and its load, and the energy reverse transmission function of AC active load are very important whether for AC motor drive, or for a new energy power grid distributed generation system, active power filter and reactive power compensation and so on. No matter which kind of the load is, the CT-ZCS inverter can automatically transfer the energy from the AC side to the DC side under the condition that the power switching control timing does not change. This function can be accomplished via alternation working of positive and negative unit of the CT-ZCS converter. As shown in Fig. 5, when the output instantaneous voltage is positive (or negative) and the negative (or positive) unit works, the energy in C_o is fed back to the positive (negative) side of the DC side through the freewheeling path composed of L_2^- and D^- (L_2^+ and D^+). Due to the dynamic voltage tracking mechanism and the fact that C_o has the buffering function on the active energy of the load, the time when CT-ZCS inverter starts to be in the state of feedback is automatically achieved according to the need of maintaining the output voltage waveform (tracking the reference voltage waveform), regardless of the load energy swallowing-or-spitting state [17], [18].

VI. The Control Method and the Experimental Results of CT-ZCS Inverter

A dedicated adaptation control method proposed is the double-digit three-state interlocking comparison pulse density modulation (DTIC-PDM) control method. The output voltage is first sampled and the sampling result is compared with the input reference signal. Then the error signal is used as the control signal of the bailer-charge transfer frequency. The density of discrete current pulse charging the output capacitor C_o is adjusted and the output voltage tracks the changes of the input signal dynamically. The dynamic tracking of alternating input reference signal can be obtained by controlling the current pulse density and keeping the flexibility in the anti-two CT-ZCS converter unit alternation. Double-digit three-state logic signal forms the cross interlocking logical combination through a logic gate. The double-digit three-state interlocking logic variables is gained, which is used as the reset control signal of two square-wave generator, so that the switch drive pulse density of the two square wave generator output can be modulated. The maximum output frequency of the two square-wave generator determines the upper limit of the current

Fig. 7. Resonance compensation block diagram using DFT filter.

pulse density of the CT-ZCS inverter under PDM control, and also determines the maximum load short-circuit current. This method based on the nonlinear control mode with pulse density modulation on double-digit three-state logic interlock comparator is defined as double-digit three-state interlocking comparison pulse density modulation (DTIC-PDM). There are similar characteristics with the hysteresis current control and the current predictive control, i.e., a simple, reliable and fast response. Based on the AC side voltage waveform and tracking the feedback signal, organic combine according to a certain deviation tolerance, it reduces sensitivity with circuit parameter, ie, capacitor, inductance, resistance and load changes, which help to improve the robustness of the system.

To observe the inverter's dynamic voltage tracking

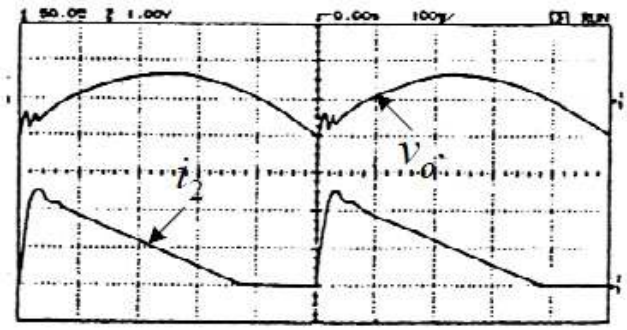

Fig. 8. The experimental waveforms of ouput voltage v_o and the current through L_2.

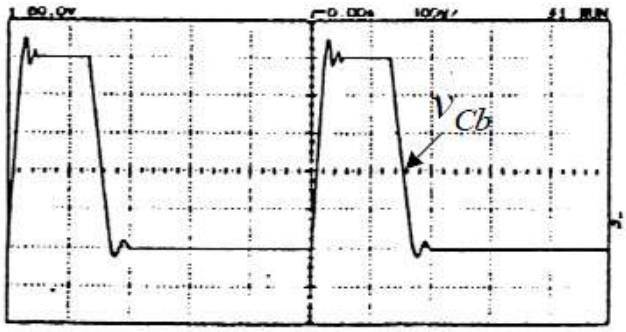

Fig. 9. The experimental waveforms of the voltage across C_b.

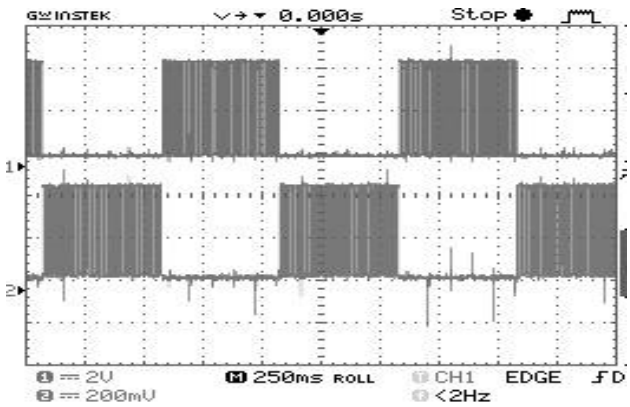

Fig. 10. The experimental waveforms of the pulse sequence on positive unit and negative unit.

performance, the experiment of the step wave voltage tracking and single-phase asynchronous motor unit frequency control have been carried out and a 1.5 kW prototype of the proposed converter has been constructed. The control circuit setup treated here is shown in Fig.6. The parameter values of CT-ZCS inverter used in this paper are: V_d=600 *V;* L_1=10 *uH*; L_2=100 *uH* and fast thyristor with 100 *A* / 1200 *V*. The experimental setup using DTIC-PDM is presented in Fig. 7.

Fig. 8-9 show the operational waveforms of Fig.1 and Fig. 10-13 show the operational waveforms of the Fig. 5. Fig. 14 shows the efficiency graph of Fig. 5. These waveforms show that the output voltage (v_o) can track the input reference signal (v_B) dynamically and replicating it in proportion to its value accurately. The power balanced relations and the power flow direction are determined by the unique coordination control method. The presented experimental results confirm the theoretical analysis provided in the previous sections.

VII. Conclusions

A new topology of CT-ZCS converters was proposed in this paper. By analyzing the equivalent topological decomposition and establishing the standardized state trajectory equation trajectory diagram, the transformation principle and working waveform were discussed, and the quantitative analysis and research on working process were conducted; the difference of

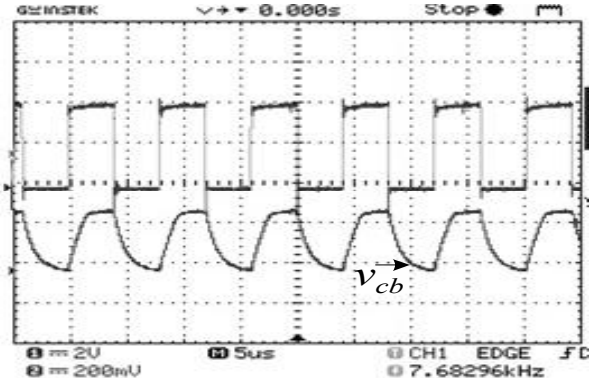

Fig. 11. The experimental waveforms of the voltage across C_b^+ and the control pulse on the S_1^+.

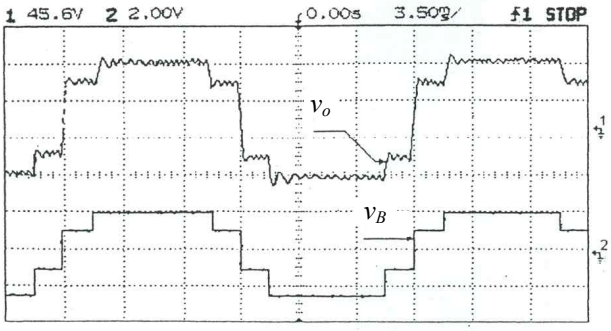

Fig. 12. The dynamic voltage tracking waveforms of step wave.

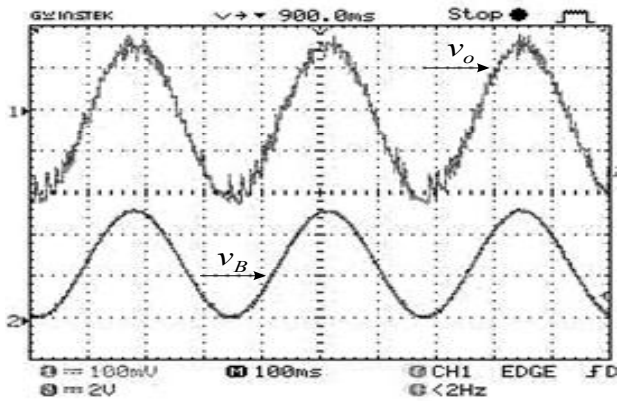

Fig. 13. The dynamic voltage tracking waveforms of sine wave.

the state trajectories between continuous current mode and discontinuous mode was researched; the switching frequency and output voltage ripple calculation methods were given, and a set of valuable design and calculation formulas were obtained. The CT-ZCS converter based on the bailer-capacitor provide many characteristics: tracking the input reference signal dynamically and replicating it in proportion to its value accurately, bearing load shock and short circuit, multiple inverter N+1 redundant parallel and power balance coordination easy control, soft-switching commutation being benefits for high efficiency and the large capacity. The advantages are distinctive from conventional inverter topologies which are especially demanded in AC drives, new

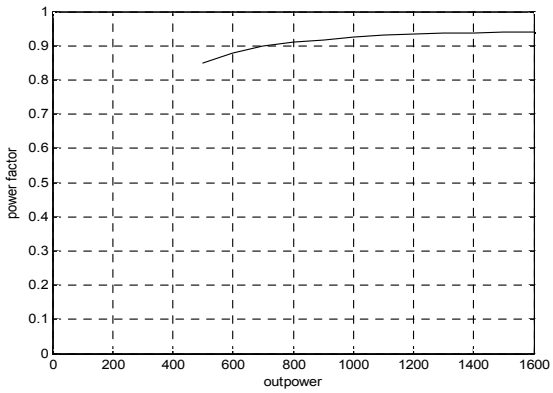

Fig. 14. The efficiency graph of CT-ZCS inverter.

energy generation and grid distributed generating systems, switching power amplifiers, active power filters, and reactive power compensation and so on. By using a unique PDM control method, the CT-ZCS inverter output voltage combined with CT-ZCS transformation mechanism and work characteristics show a good dynamic tracking features and a good analogue voltage output waveform effect on the input reference signal.

ACKNOWLEDGMENT

This work was supported in part by the Natural Science Foundation of Shandong, China (No. ZR2009FM008), and in part by the science and technology r&d program of Shandong, China(No. 2010GGX10714).

REFERENCES

[1] G. Pawan and P. Amit, "Hybrid mode-switched control of DC-DC boost converter circuits," *IEEE Trans. Circuits Syst. II, Exp. Briefs*, Vol. 51, No. 11, pp. 734-738, Nov. 2005.

[2] Q. Z. Zhou and X. D. Liu, "Switch-Linear hybrid (SLH) conversion based on source follower," *IEEE Trans. Power Electron.*, Vol. 23, No. 5, pp. 2399-2410, Sep. 2008.

[3] S. Nitesh and P. Sudhakar, "A digital envelope combiner for switching power amplifier linearization," *IEEE Trans. Circuits Syst. II, Exp. Briefs*, Vol. 57, No. 4, pp. 270-274, Apr. 2010.

[4] D. L. Chen and Y. J. Zhang, "Research on uni-polarity phase shifting controlled inverters with high frequency pulse AC link," *Proceedings of the Chinese Society of Electrical Engineering*, Vol. 23, No. 4, pp. 27-30, Apr. 2003.

[5] P. T. Krein, R. S. Balog, and X. Geng, "High-frequency link inverter for fuel cells based on multiple-carrier PWM," *IEEE Trans. Power Electron.*, Vol. 19, No. 5, pp. 1279-1288, Sep. 2004.

[6] T. Mishimay, E. Hiraki, and M. Nakaoka, "A high frequency-link bidirectional DC-DC converter for super capacitor-based automotive auxiliary electric power systems," *Journal of Power Electronics*, Vol. 10, No. 1, pp. 27-33, Jan. 2010.

[7] M. Jabbari and H. Farzanehfard, "Family of soft-switching resonant DC-DC converters," *IET Power Electronics*, Vol. 2, No. 2, pp. 113-124, Mar. 2009.
[8] I. D. Kim, J. Y. Kim, E. C. Nho, and H. G. Kim, "Analysis and design of a soft-switched PWM sepic DC-DC converter," *Journal of Power Electronics*, Vol. 10, No. 5, pp. 461-467, Sep. 2010.
[9] L. L. Chen, Y. H. Xu, and B. Zhou, "Research on series resonant DC/DC converter based on variable-frequency control," *Advanced Technology of Electrical Engineering and Energy*, Vol. 30, No.3, pp. 6-9, Mar. 2011.
[10] W. W. Burns, "A state-trajectory control law for DC-to-DC converters," *IEEE Trans. Aerosp. Electron. Syst.*, Vol. 14, No. 1, pp. 2-20, Jan.1978.
[11] T. T. Song and H. S. H. Chung, "Boundary control of boost converters using state-energy plane," *IEEE Trans. Power Electron.*, Vol. 23, No. 2, pp. 551-564, Mar. 2008.
[12] K. K. S. Leung and H. S. H. Chung, "Dynamic hysteresis band control of the buck converter with fast transient response," *IEEE Trans. Circuits Syst. II, Exp. Briefs*, Vol. 52, No. 7, pp. 398-402, Jul. 2005.
[13] C. N. M. Ho, V. S. P. Cheung and H. S. H. Chung, "Constant-Frequency hysteresis current control of grid-connected VSI without bandwidth control," *IEEE Trans. Power Electron.*, Vol. 24, No. 6, pp. 2484-2495, Nov. 2009.
[14] Z. R. Lai and K. M. Smedley, "A new extension of one-cycle control and its application to switching power amplifiers," *IEEE Trans. Power Electron.*, Vol. 11, No. 1, pp. 99-105, Jan. 1996.
[15] Y. S. Lee and G. T. Cheng, "Quasi-resonant zero-current-switching bidirectional converter for battery equalization applications," *IEEE Trans. Power Electron.*, Vol. 21, No. 5, pp.1213-1224, Sep. 2006.
[16] H. Ertl, and J. W. Kolar, and F. C. Franz, "Basic considerations and topologies of switched-mode assisted linear power amplifiers," *IEEE Trans. Power Electron.*, Vol. 12, No. 1, pp. 116-123, Jan. 1997.
[17] G. R. Walker, "A class B switch-mode assisted linear amplifier," *IEEE Trans. Power Electron.*, Vol. 18, No. 6, pp. 1278-1285, Nov. 2003.

Rong Chen was born in Shandong, China, in 1976. He received the B.S. degree in industrial automation, in 1998, and the M.S. degree in control theory and control engineering, in 2001, from the Shandong University of Science and Technology, Shandong, China. He is currently working toward the Ph.D. degree in control theory and control engineering at the China University of Petroleum (UPC). His research interests include electric machine drives, power electronics, high frequency soft switching converters, and power factor correction.

Jia-Sheng Zhang was born in Shandong, China, in 1957. He received the B.S. degree in applied electronic technology from China University of Petroleum, Shandong, China, in 1982, and the M.S. and Ph.D. degrees in electrical and electronic engineering from Beijing Jiaotong University, Beijing, China, in 1988 and 1998, respectively. In 1982, he joined the Department of Electrical Engineering, China University of Petroleum, Shandong, China, where he is currently a full-time Professor. His current research interests include power electronics, motor drives, power quality control, renewable distributed power sources, and DSP-based control of power converters.